

Modeling and Analysis of a LOX/Ethanol Liquid Rocket Engine

Fábio Antônio da Silva Mota¹, José Nivaldo Hinckel², Evandro Marconi Rocco², Hanfried Schlingloff³

Mota FAS  <http://orcid.org/0000-0003-3672-0547>

Hinckel JN  <http://orcid.org/0000-0002-0171-2697>

Rocco EM  <http://orcid.org/0000-0003-0660-0587>

Schlingloff H  <http://orcid.org/0000-0003-1806-9113>

How to cite

Mota FAS; Hinckel JN; Rocco EM; Schlingloff H (2018) Modeling and Analysis of a LOX/Ethanol Liquid Rocket Engine. J Aerosp Techno Manag, 10: e3018. doi: 10.5028/jatm.v10.914.

ABSTRACT: This work studies the performance and dry mass of the under development LOX/Ethanol L75 liquid rocket engine. To this end, an object-oriented program written in C++ was developed. The program is intended to be versatile and easily extensible in order to analyze different configurations of liquid rocket engines. The UML (Unified Modeling Language) tool is used to model the architecture of the codes. UML diagrams help to visualize the code structure and the communication between objects, enabling a high degree of abstraction. The cryogenics Vulcain and HM7B engines power cycles along with the staged-combustion SSME engine perform the verification of the codes. Finally, the influence of changes in design parameters on the performance and dry mass of the L75 rocket engine is analyzed.

KEYWORDS: Liquid rocket engines, Ethanol, Modeling.

INTRODUCTION

A liquid rocket engine can be divided into feed system and thrust chamber assembly. The feed system is responsible to lead the propellants to the thrust chamber providing enough pressure energy to overcome all pressure losses in the lines and components and reaching the established combustion chamber pressure. To provide such pressure energy, pressure-fed and turbopump fed system are the options available for launch vehicles technology. The turbopump assembly (TPA) is designated to deliver the required energy to the propellants. Although many configurations of turbopump fed cycle can be found in the literature, most of them are derived from the traditional gas generator cycle (GG), staged combustion (SC), and expander cycle (EC). Another way to categorize the engine cycles is based on the turbine and thrust chamber arrangement. In other words, the cycles can be classified as open or closed. In an open cycle, the turbine is in parallel with the thrust chamber, and the drive gases are either dumped overboard or injected in the divergent section of the nozzle.

The Brazilian space program has been aimed at launch vehicles using solid propellants with launch capability limited to a few hundred kilograms into Low Earth Orbit (LEO). To enlarge the launch envelope and also to improve the launch injection accuracy, rocket engines driven by liquid propulsion are not an option, but a must. A program for the development of a liquid rocket engine is currently being carried out at the Brazilian Aeronautics and Space Institute (IAE) in cooperation with the German Aerospace

¹.Universidade Federal do ABC – Centro de Engenharia, Modelagem e Ciências Sociais Aplicadas – Departamento de Engenharia Aeroespacial – Santo André/SP – Brazil | ².Instituto Nacional de Pesquisas Espaciais – Departamento de Engenharia e Tecnologia Espacial – São José dos Campos/SP – Brazil | ³.Ostbayerische Technische Hochschule Regensburg – Department of Mechanical Engineering – Regensburg – Germany.

Correspondence author: Fábio Antônio da Silva Mota | Universidade Federal do ABC – Centro de Engenharia, Modelagem e Ciências Sociais Aplicadas – Departamento de Engenharia Aeroespacial | Av. dos Estados, 5001 | CEP: 09.210-580 – Santo André/SP – Brazil | E-mail: mota.fabio@ufabc.edu.br

Received: Mar. 8, 2017 | Accepted: Jul. 11, 2017

Section Editor: Carlos Marchi



Center (DLR), to be used in the upper stage of the Brazilian launch vehicle. The idea is to replace the last two solid stages of the VLS-1 launch vehicle by a single liquid rocket stage. The LRE, named L75, will be capable of reaching a thrust range of (75 ± 5) kN using the propellants combination LOX/Ethanol. During the simulations and trade-off studies phase, the availability of a versatile tool for this purpose is very useful. One of the most important and robust tools for vehicle/propulsion analysis was developed when the German Aerospace Center (DLR) and NASA combined computer codes to provide a capability to optimize rocket engines cycles and its parameters, as well as launch vehicles, considering the coupling between them. In many publications you can find applications of this tool (Manski and Martin 1990; 1991; Goertz 1995; Manski *et al.* 1998; Burkhardt *et al.* 2002; 2004; Sippel *et al.* 2003; 2012).

The aim of this paper is to give a preliminary analysis of the L75 rocket engine operating at design and off-design conditions. To this end, an object-oriented program written in C++ capable of analyzing multiple configurations of liquid rocket engines is developed. Another purpose of this paper is to present a detailed description of the main components (design equations, main parameters, restrictions, etc.) and the physical laws necessary to balance any power cycle.

COMPONENTS MODELING

The common components for most of the turbopump-fed liquid rocket engines (LRE) are pumps, turbine(s), valves, pipes, and thrust chamber. Depending on its configuration, a gas generator (for gas generator cycle), a pre-burner(s) (for staged combustion cycle) and booster-pumps can be found as well. This section presents the modeling of the main components of a liquid rocket engine that will be used to model the power cycle. In addition to the design equations, the design parameters, limitations and restrictions of each component are discussed.

TURBOPUMP

The turbopump assembly (TPA) is required when it is desired a higher pressure in the combustion chamber, i.e., when we are dealing with launch vehicles. Usually if the density of the propellants are relatively close, an arrangement with single shaft TPA can be applied. However, if the propellants have strongly different densities, as the case of the LOX/LH2 combination, a dual shaft TPA – a TPA with two turbines with configurations working in series or in parallel – is required. There is still a configuration using gear case, which implies in a more complicated design, then, a single shaft TPA is commonly preferred.

Pump

For space application, weight is a key parameter, so centrifugal pumps are preferred because they can handle a large amount of mass flow rate. Nevertheless, axial and mixed pumps are used. The required pump mass flow is parameterized by the engine design parameters: thrust, effective exhaust velocity, mixture ratio, and propellant densities. Assuming steady flow, the pump basically increases the Bernoulli head between the pump inlet and exit (Eq. 1) (White 1998):

$$H_p = \left(\frac{P}{\rho g_0} + \frac{v^2}{2g_0} + z \right)_{discharge} - \left(\frac{P}{\rho g_0} + \frac{v^2}{2g_0} + z \right)_{inlet} \quad (1)$$

where: H_p = pump head rise (m); g_0 = standard gravitational acceleration (9.81 m/s^2).

For a liquid rocket engine the terms in the right side, related to kinetic ($v^2/2g_0$) and potential energy (z), can be neglected, so the net pump head is essentially equal to the change in pressure head (Eq. 2):

$$H_p = \frac{P_d - P_t}{g_0 \rho} \quad (2)$$

where: p_d = discharge pressure (Pa); p_i = inlet pressure (Pa); ρ = density of the working fluid (kg/m^3). The required pump power is given by (Humble *et al.* 1995):

$$P_p = \frac{g_0 \dot{m} H_p}{\eta_p} \quad (3)$$

where: P_p = pump power (J/s), \dot{m} = propellant mass flow rate (kg/s); η = efficiency (-).

The required pump power is a key parameter to balance the cycle. Since Eq. (3) was derived for incompressible flow, substantial deviations from the predictable values can be found when a relatively high pressure is applied to a low density propellant (e.g., liquid hydrogen) as will be seen in the results for the Vulcain and SSME rocket engines. For those cases, the pump power can be calculated in terms of enthalpy change Δh (Eq. 4):

$$P_p = \frac{\dot{m} \Delta h}{\eta_p} \quad (4)$$

where: h = enthalpy (J / kg).

A similarity parameter that characterizes pumps and influences the pump's hydraulic efficiency η_p is the stage-specific speed N_s (Eq. 5) (Humble *et al.* 1995):

$$N_s = \frac{N_r \sqrt{Q}}{(H_p / n)^{0.75}} \quad (5)$$

where: N_r = rotational speed of the pump (rad/s); Q = volume flow rate (m^3/s); n = number of pump stages (-). In this work, the efficiency of the pump is a parameter given by the user. Using N_s , White *et al.* (1995) present a method to easily estimate pump's efficiency.

Turbine

The turbine is a device that extracts energy from a flowing working fluid, which can be combustion gases from a gas generator, a pre-burner, or even warm gases leaving the cooling jacket in an expander cycle. For an auxiliary turbopump arrangement, hydraulic turbines, which derive its energy from liquid propellant coming from the main pump, can also be found. Ideally, there are two types of axial-flow turbines of interest to rocket pump drives: impulse turbines and reaction turbines. The power of the turbine can be determined by (Eq. 6):

$$P_T = \eta_T \dot{m}_T \Delta h \quad (6)$$

where P_T = turbine power (J/s).

The turbine pressure ratio is defined as (Eq. 7):

$$p_{Tr} = \frac{p_{Ti}}{p_{Td}} \quad (7)$$

where: p_{Tr} = turbine pressure ratio; and the indexes Ti , and Td refer to turbine inlet and turbine discharge, respectively. If we assume that the specific heat c_p and the ratio of specific heats γ are constant during the expansion of gases, the power of the turbine can be given in an alternative form (Eq. 8):

$$P_T = \eta_T \dot{m}_T c_p T_i \left[1 - \left(\frac{1}{p_{Tr}} \right)^{(\gamma-1)/\gamma} \right] \quad (8)$$

where: T_i is the turbine inlet temperature.

In this work, the parameters Δh , c_p , and γ from Eqs. 6 and 8 are calculated using the well-known CEA program (Gordon and McBride 1994; 1996). However, the CEA program can be used only for a gas turbine driven by gases from combustion. For example, in the expander cycle, the turbines are driven by hot gases from the heat exchanger, and booster pumps can be driven by hydraulic turbines, thus in these cases only Eq. 6 can be used and the enthalpy change will be a parameter given by the user.

As well as the pump has a parameter (stage-specific speed) that can be used to estimate its efficiency, the turbine has the theoretical gas spouting velocity C_0 (m / s). A method to estimate the efficiency of the turbine based on C_0 is presented in Humble *et al.* (1995). The spouting velocity derived from enthalpy drop is defined as that velocity which will be obtained during an isentropic expansion of the gas from the turbine inlet conditions to the turbine exit static pressure at the rotor blade inlet (Eq. 9) (Humble *et al.* 1995; Huzel and Huang 1992):

$$C_0 = \sqrt{2c_p T_i \left[1 - \left(\frac{1}{p_{Tr}} \right)^{(\gamma-1)/\gamma} \right]} \quad (9)$$

Booster Turbopump

In a few applications, in order to prevent cavitation in the main pump, an increase in pump inlet pressure can be carried out. To this end, the propellant tanks pressure can be increased, or an auxiliary turbopump can be installed. The first option implies an extra structural mass of the tanks. So, in order to minimize the structural mass, the second approach is usually chosen. According to Sutton and Biblarz (2010), a typical booster-turbopump can provide about 10% of the required pump pressure rise, then the main pump would be responsible for the remaining 90%. Important applications of booster-turbopumps can be seen in the American Space Shuttle Main Engine (SSME) and the Russian RD-170.

THRUST CHAMBER

The thrust chamber assembly consists of combustion chamber, nozzle and igniter. In the thrust chamber, the propellants that come from the feed system are injected, atomized, mixed and burned to turn into hot gases that are ejected at high speeds. By the principle of conservation of energy, it can be understood that in the thrust chamber occurs a conversion of random motion of the molecules at high speeds (heat) into an ordered stream of gas at high speed (kinetic energy). The thrust equation can be derived from Newton's Second Law, which states that for an inertial reference frame the net force is equal to rate of change of momentum (product of the velocity and mass). In a rocket, the flow of gases from combustion causes a reaction force (thrust) on the structure, thus (Eq. 10):

$$F = \eta_c \eta_{ne} [\dot{m} v_e + (p_e - p_a) A_e] \quad (10)$$

where: F = thrust force (N); v_e = nozzle exit velocity of gases (m / s). v_e can be estimated by applying an energy balance (Eq. 11):

$$v_e = \sqrt{v_i^2 + 2(h_i - h_e)} \quad (11)$$

Another way to estimate the thrust force can be achieved by the main rocket performance parameters, namely: specific impulse, effective exhaust velocity, characteristic velocity, and thrust coefficient. For example, the specific impulse I_{sp} (s), which is defined as the total impulse per unit weight of the propellant for steady flow, can be given as (Eq. 12):

$$I_{sp} = \frac{F}{g_0 \dot{m}} \quad (12)$$

GAS GENERATOR OR PRE-BURNER

The gas generator and the pre-burner operate exactly in the same way. They are responsible to burn an amount of propellant in order to drive the turbine(s) by means of gases from combustion. The difference between them is that the gas generator is applied for open cycle engines, while the pre-burner performs a first stage of combustion, i.e., this mixture is not dumped off, but completely burned in the combustion chamber.

To obtain the properties of the gases from combustion, the CEA program is used. However, it is important to point out that CEA does not work properly with long organic molecules when used in fuel rich application. This problem was also verified by Kauffmann *et al.* (2001), and a method was presented to circumvent this limitation.

INJECTOR HEAD

The injector is responsible to accelerate the propellants through small holes in order to atomize them inside the combustion chamber. As a rule thumb, the pressure drop across injector head Δp_{inj} is some percentage of the chamber pressure (Eq. 13) (Humble *et al.* 1995):

$$\Delta p_{inj} = \begin{cases} 0.20 p_c, & \text{if unthrottled} \\ 0.30 p_c, & \text{if throttled} \\ 0.05 p_c, & \text{if pintle-type} \end{cases} \quad (13)$$

Some amount of pressure drop is desirable to isolate chamber-pressure oscillations from the feed system, reducing coupling between the combustion chamber and the feed system. An alternative relation can be given as (Eq. 14) (Kesaev and Almeida 2005):

$$\Delta p_{inj} = \begin{cases} 0.8 \times 10^2 \sqrt{10 p_c}, & \text{if liquid propellant} \\ 0.4 \times 10^2 \sqrt{10 p_c}, & \text{if gas propellant} \end{cases} \quad (14)$$

where: p_c is given in (Pa).

A detailed modeling of the injector is not within the scope of this work. Only the pressure drops, which can be user defined or given by the correlations above (rough estimation), are of interest in this work.

HEAT EXCHANGER

The heat exchanger (or cooling system) is responsible to absorb heat from the walls of the thrust chamber in order to prevent the wall material from change phase, i.e., the material can be melted or even evaporated. The most used and efficient for a LRE is the regenerative cooling system where the working fluid (usually the fuel) exchanges heat from the thrust chamber and then the fluid is burned in the combustion chamber. With this cooling system all heat absorbed can be used for purposes of propulsion, hence the name regenerative. Another common cooling system is the so-called dump cooling, which drop off at supersonic speeds the propellant overboard. Because of such a high speed, normally a small portion of thrust is generated. Although the propellant remains unburned, the heated propellant can give very reasonable values of specific impulse, therefore the negative impact on the overall specific impulse is little, if any (Pavli and Curley 1996). According to Humble *et al.* (1995), pressure drops in the cooling jacket Δp_{cool} can vary between 10% and 20% of the chamber pressure p_c . Then, for preliminary analysis, the authors suggest (Eq. 15):

$$\Delta p_{cool} = 0.15 p_c \quad (15)$$

In Kesaev and Almeida (2005) the following correlations are found (Eq. 16):

$$\Delta p_{cool} = \begin{cases} (0.25 - 0.30)p_c, & \text{if } p_c < 80 \text{ MPa} \\ (0.30 - 0.35)p_c, & \text{if } p_c > 80 \text{ MPa} \end{cases} \quad (16)$$

In this work, Δp_{cool} is an input parameter given by the user, but if no input is given, it will be used a simple relation function of the chamber pressure as the ones previously presented.

PIPE SYSTEM: FEED LINES AND VALVES

The feed system is responsible to conduct the propellants to the thrust chamber providing enough pressure energy to overcome all the pressure losses in the lines and components and reaching the established combustion chamber pressure (p_c). The required pump discharge pressure is determined from the chamber pressure and the hydraulic losses in valves, lines, cooling jacket, and injector head. To obtain the rated flow at the rated pressure, an additional adjustable pressure drop for a flow orifice is usually included, which permits a calibration adjustment or change in the required feed pressure (Sutton and Biblarz 2010). For a gas generator cycle, the stagnation pressure drop of the propellants between the pump discharge and the combustion chamber is the sum of pressure drop in pipes, valves, elbows, cooling system (for the fuel), and injectors (Eqs. 17 and 18).

$$p_{pump,f} - p_c = \Delta p_{f,lines} + \Delta p_{f,valves} + \Delta p_{f,cool} + \Delta p_{f,inj} \quad (17)$$

$$p_{pump,o} - p_c = \Delta p_{o,lines} + \Delta p_{o,valves} + \Delta p_{o,inj} \quad (18)$$

Relations that are functions of chamber pressure can estimate the pressure drops in the right side of the equations. Kesaev and Almeida (2005) present the following relation for the pressure drop through the hydraulic lines (Eq. 19):

$$\Delta p_{lines} = (0.05 - 0.1)p_c \quad (19)$$

and for duct gas (section between turbine and thrust chamber for a closed engine cycle) (Eq. 20):

$$\Delta p_{duct}^{gas} = \begin{cases} 0.025 p_c \\ 0.15 p_c, & \text{for distribution grid} \end{cases} \quad (20)$$

In this paper, all pressure drops through the feed system are user input, but if no value is given, the simple relations previously presented are assumed. Because of the lack of data about the feed system dimensions, such as length of pipes, number of elbows, and so on, a detailed modeling of the feed system is out of scope of work.

MASS MODELING

There are numerous relations for estimating engine and stage mass in the literature. Most of them are based on historical and empirical data, as we can see in Felber (1979), Schlingloff (2005) and Ernst (2014) in turn taken from Zandbergen (2013). The mass and dimensions of existing and historical liquid rocket systems (excluding tanks) correlate well with thrust magnitude. From mission-level analysis, we know how much thrust we need, so we can easily estimate system mass (Humble *et al.* 1995). Using a database with 51 LRE, Castellini (2012) analyzed linear, quadratic, power law and logarithmic curves. The best resulting regression in terms of quadratic fit error for each technology were implemented within the propulsion models. Another way to estimate the engine mass is to calculate from empirical models the mass of the main components of the engine, and then to make use of regression techniques to fit a curve to data obtained from historical rocket engines. Considering propellant type, feeding cycle, chamber pressure, and nozzle expansion ratio, Schlingloff (2005) proposed the model showed in Eq. 21:

$$m_{eng} = 1.34(m_{tp} + m_{valve} + m_{inj} + m_{cc} + m_{ne}) \tag{21}$$

where: $m_{tp} = C_{propellant} \cdot C_{tp} (F \cdot p_c)^{0.71}$; $m_{valve} = 0.02 (F \cdot p_c)^{0.71}$; $m_{inj} = 0.25 F^{0.85}$; $m_{cc} = 0.75 F^{0.85}$; $m_{ne} = \epsilon F (0.00225 C_{nozzle} + (0.225 - 0.075 C_{nozzle})) / p_c$. $C_{propellant} = 0.19$, if high energetic propellant, and 0.11, if low energetic propellant. $C_{tp} = 0.5$, if boost-pumps, and 1.0, if no boost-pumps. $C_{nozzle} = 1.0$, if regenerative cooling, and 0.0, if dump cooling. The mass has dimensions of kilograms, the vacuum thrust F of the engine is specified in kN and the chamber pressure p_c in bar. In this model, the mixture ratio r_c has no influence. Thus, in order to take it into account, we can replace the turbopump equation with a more generic equation (Eq. 22) (Felber 1979):

$$m_{tp} = \frac{0.178}{k_{tp}} \rho^{0.148} P_T^{0.73} \tag{22}$$

where: $k_{tp} = 1$, if no boost-pumps, and 2, if boost-pumps.

This equation is valid for power varying between 300 and 6×10^4 kW. As the turbopump mass equation was modified, the correction factor in Eq. 21 is no longer valid. To determine a new correction factor, the rocket engines HM7B, HM60, Le-5, J-2, H-1, and RS-27 were considered (Table 1). The correction factor was determined by linear regression of the actual values of the main components versus the calculated ones, thus the new model takes the form:

$$m_{eng} = 1.59921(m_{tp} + m_{valve} + m_{inj} + m_{cc} + m_{ne}) \tag{23}$$

The Eq. 23 represents a so-called analytical/statistical model, which means it considers not only statistical data but also physical relationships. This model is sufficiently detailed when the influence of the engine parameters on the engine mass or payload mass are aim of study.

Table 1. Mass model validation.

| LRE | Propellant | Actual (kg) (Mc Hugh 1995) | Calculated (kg) | Error |
|-------|------------|----------------------------|-----------------|-------|
| HM7B | LOX/LH2 | 158.0 | 167.2 | 5.8 |
| HM60 | LOX/LH2 | 1719.0 | 1809.2 | 5.2 |
| LE-5 | LOX/LH2 | 255.0 | 324.2 | 27.1 |
| J-2 | LOX/LH2 | 1542.0 | 1440.4 | 6.6 |
| H-1 | LOX/RP-1 | 878.2 | 932.2 | 6.2 |
| RS-27 | LOX/RP-1 | 1146.6 | 1060.7 | 7.5 |

CYCLES MODELING

This section describes a methodology to model and simulate power cycles of liquid rocket engine operating under steady-state condition. Although many methods and tools (both commercial and in-house) to model and simulate power cycles do exist, there are not many available works in the open literature. This fact is presumably due to sensitive technology characteristic.

BALANCE EQUATIONS

To simulate a liquid rocket engine it is necessary to make use of conservation laws to balance the cycle. Mass balance, power balance of the turbopump(s), pressure balance through the lines, and the momentum equation can define a set of nonlinear algebraic equations. For each type of cycle, turbopump arrangement, and split flows or bypass, a different set of equations can be stated. To perform the simulation the following considerations will be taken into account:

- The propellants flow under steady state condition
- The liquid propellants behave as incompressible fluid
- There is no heat loss to the environment
- There is no variation of the temperature in the pipes

Flow and Energy Balance

Depending on the turbopump arrangement a different power balance can be established. In this work, it will be distinguished among four types of turbopumps, namely: single shaft, geared, dual shaft with turbines in series, and with turbines in parallel.

The required pump discharge pressure p_d is determined by the chamber pressure and the hydraulic losses through the feed system. In order to obtain the rated flow at the rated pressure, usually a flow orifice is conveniently added. It adjusts the pressure drop, which permits a calibration adjustment or change in the required feed system pressure. For a gas generator cycle, the stagnation pressure drop of the propellants between the pump discharge and the combustion chamber is the sum of pressure drops in feed lines, valves, cooling system (for the fuel), and injectors. For closed cycles in which the turbine(s) is in series with the thrust chamber there is an extra pressure drop through the turbine.

Flow Splitter

A flow splitter is used to divide a given flow stream in two branches. The reason to split a flow arises from applications from cooling system to thrust control. For example, an expander cycle makes use of a bypass around the turbine to control the thrust.

Input Parameters

The formulation of the set of equations can also be modified depending on the input and output parameters. For example, in order to close the balance of the thermodynamic cycle, the user can select the net thrust force or the overall mass flow rate can be as input parameters.

SET OF NON-LINEAR EQUATIONS – SOLVER

To simulate a LRE cycle, mass and energy conservation laws must be fulfilled. Components mass balance, power balance of turbopumps, pressure balance, and a momentum balance or a global mass balance can define a nonlinear set of equations. For each type of cycle and its arrangements a different set of equations can be stated. Thus, if we define a set of unknown x_i and an equal number of independent equations f_i , a nonlinear system of equation can be written as (Eq. 24):

$$\begin{aligned} f_1(x_1, x_2, \dots, x_N) &= 0 \\ f_2(x_1, x_2, \dots, x_N) &= 0 \\ &\vdots \\ f_N(x_1, x_2, \dots, x_N) &= 0 \end{aligned} \quad (24)$$

To solve this numerical problem, the Newton's method or the multidimensional secant methods called Broyden's method can be used. The routines used in this work were taken from the book of Press *et al.* (2007).

PROGRAMME SETUP

This section describes the general architecture of the application program. As previously mentioned, a modular approach using object-oriented programming (OOP) is chosen and, to allow a better visualization of the codes, UML diagrams are used. The mathematical models developed in the previous sections will be part of the functionality of each code module. Usually, OOP is not the first option for engineers or researchers, in part because they are already relatively acquainted with procedural programming and also because of the inherent complexity to deal with objects. In fact, the task of creating a well-designed class hierarchy describing

a complex rocket system is quite challenging. Besides, the class interface and its functionality do not proceed in a straightforward manner, but require many trial and error and rearrangement Hinckel (1995). UML is a tool for modeling object-oriented codes. It is used to visualize the code and the communication between objects enabling a high degree of abstraction. In the following section, the way components of a LRE can be grouped in order to create a subsystem or system is outlined. In short, the use of UML diagrams will facilitate the communication among components of a LRE.

UML SCHEMES OF LIQUID ROCKET ENGINES

Figure 1 presents a possible UML diagram for a liquid rocket engine with gas generator cycle and single shaft turbopump. The configuration of the diagram was conveniently chosen to represent the L75 rocket engine. From the diagram we can see some parameters and functions of each component and the relationship between them. In order to make the diagrams clearer, some parameters and functions are omitted. The rocket engine is compound of objects of the following components (classes): Turbopump, ThrustChamber, Valves, GasGenerator and LiquidPropellant. These objects along with specific impulse, thrust force, mixture ratio, and feed lines pressure drops compose the parameters of the rocket engine (LiquidRocketEngine class). The functionality of each block was presented in previous sections.

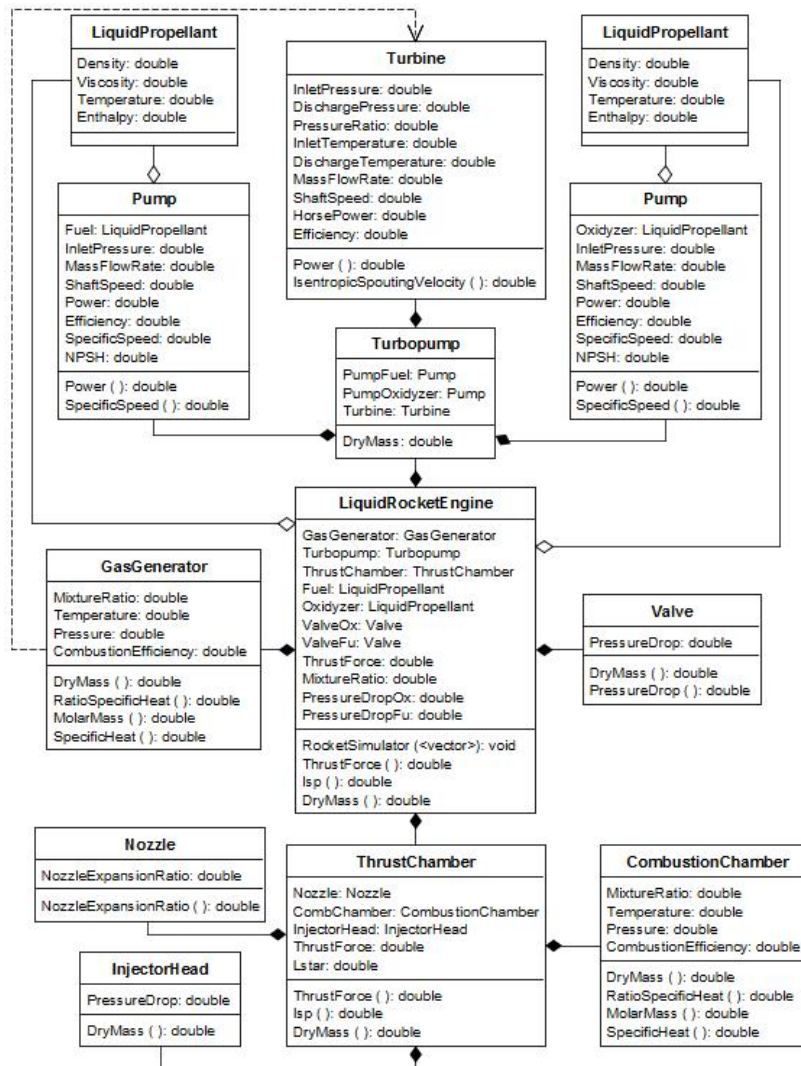


Figure 1. UML diagram of a gas generator cycle.

The dashed arrow between gas generator and turbine represents the dependency of turbine functionality on gas generator functions, i.e., the function $Power()$ depends on combustion gas parameters which are functions of the gas generator class.

RESULTS

Taking the operational open cycles Vulcain and HM7B engines, and also the closed cycle SSME rocket engine, the efficiency and applicability of the developed codes are verified. Finally, a simplified analysis of the L75 rocket engine working at different operating points is presented.

PREDICTION OF PERFORMANCE OF LIQUID ROCKET ENGINES

Vulcain

The European Vulcain, used as the core engine by Ariane 5, operates with gas generator cycle. Differently from the L75, the Vulcain has one turbine for each one of the propellants due to the relatively large difference of densities between its propellants LOX/LH2. It implies in one more unknown (mass flow rate through the second turbine) in the system of equations, which in turn has one more equation in order to make the system possible. The inputs necessary to solve the problem and outputs are shown in Fig. 2. A comparison with values from the literature is given in Table 2.

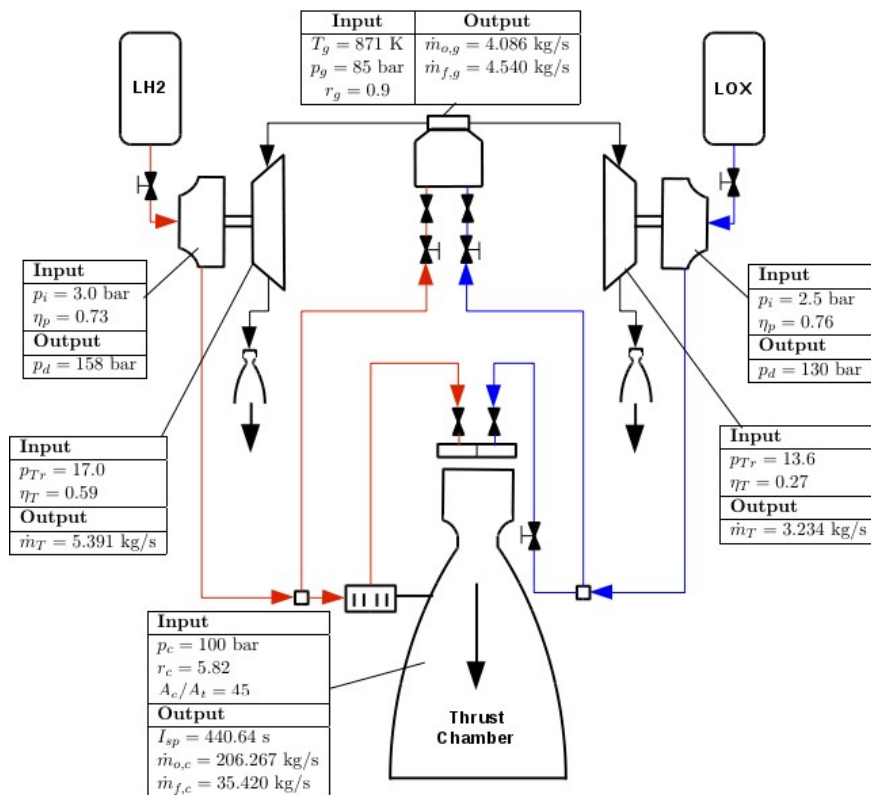


Figure 2. Vulcain flow scheme with input/output data (input data from Pouliquen 1984 and Mc Hugh 1995).

The major discrepancy was observed for the power of the fuel turbine (7.63%). The reason for that has already been discussed previously, saying that Eq. 3 can substantially deviate from the expected values when used for a low density fluid under extremely high pressure.

Table 2. Verification of the simulated parameters of the Vulcain.

| Vulcain | Actual (Pouliquen 1984; Mc Hugh 1995) | Calculated | Error (%) |
|------------------------|--|------------|-----------|
| Key input | | | |
| F (kN) | 1025 | - | - |
| p_c (bar) | 100 | - | - |
| r_c | 5.9 | - | - |
| A_e/A_t | 45 | - | - |
| Output | | | |
| I_{sp} (s) | 433.5 | 433.291 | 0.05 |
| \dot{m}_g (kg/s) | 8.4 | 8.625 | 2.68 |
| $\dot{m}_{T,o}$ (kg/s) | - | 3.234 | - |
| $\dot{m}_{T,f}$ (kg/s) | - | 5.391 | - |
| $\dot{m}_{o,c}$ (kg/s) | 198.0 | 206.267 | 4.17 |
| $\dot{m}_{f,c}$ (kg/s) | 34.0 | 35.420 | 4.18 |
| $P_{T,o}$ (MW) | 3.0 | 3.13 | 4.33 |
| $P_{T,f}$ (MW) | 11.2 | 12.054 | 7.63 |

HM7B

The European HM7B is another example of a gas generator cycle. It is used to power the upper stage of the Ariane rocket family. A geared turbopump is responsible to provide the necessary energy to the cryogenic propellants LOX/LH2. As in the case of the L75, the HM7B has only one turbine. The input and outputs are shown in Fig. 3 and Table 3.

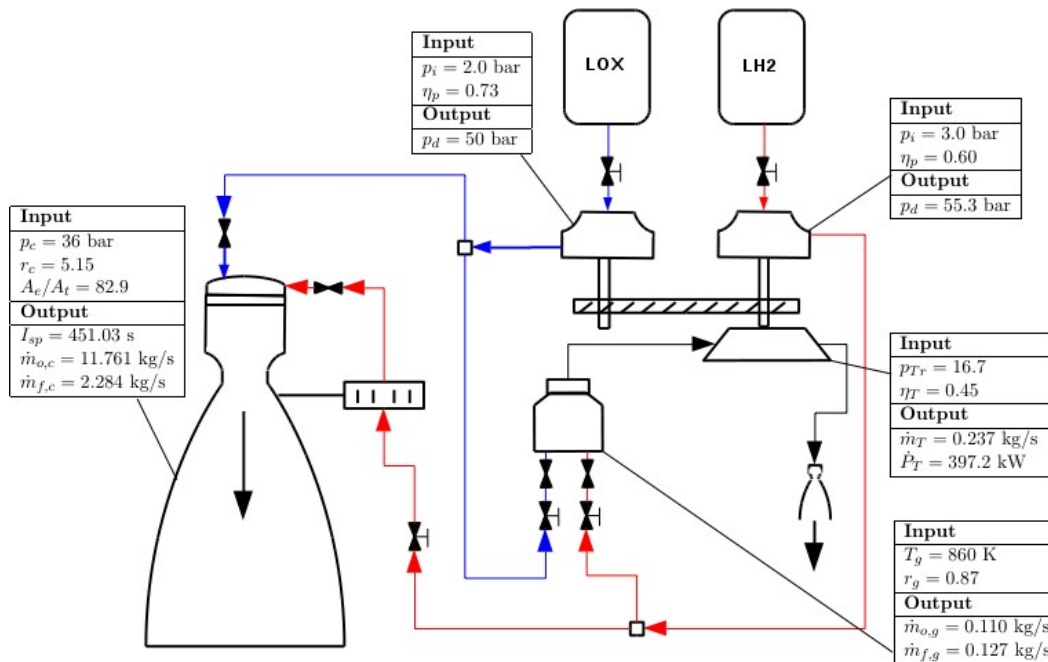


Figure 3. HM7B input/output (input data from Mc Hugh 1995).

Table 3. Verification of the simulated parameters of the HM7B.

| HM7B | Actual (Mc Hugh 1995) | Calculated | Error [%] |
|--------------------|-----------------------|------------|-----------|
| Key input | | | |
| F (kN) | 62.2 | - | - |
| p_c (bar) | 36 | - | - |
| r_c | 5.15 | - | - |
| A_c / A_t | 82.9 | - | - |
| Output | | | |
| I_{sp} (s) | 445.5 | 451.03 | 1.24 |
| $p_{d,o}$ (bar) | 50.2 | 50 | 0.40 |
| $p_{d,f}$ (bar) | 55.5 | 55.3 | 0.36 |
| \dot{m}_g (kg/s) | 0.25 | 0.237 | 5.2 |
| \dot{m}_T (kg/s) | 0.25 | 0.237 | 5.2 |
| \dot{m}_c (kg/s) | 13.9 | 14.045 | 1.04 |
| P_T (kW) | 404 | 397.2 | 1.68 |

The results show an excellent agreement with the actual values.

SSME

The Space Shuttle Main Engine (SSME) was the core engine responsible to power the Space Shuttle. Each of the two main turbopumps (HPOTP and HPFTP) is driven by a fuel-rich pre-burner. To increase the inlet pressure of both main pumps, booster turbopumps are used. Figure 4 presents the inputs and the main results obtained from the simulation. Table 4 compares the results with the literature.

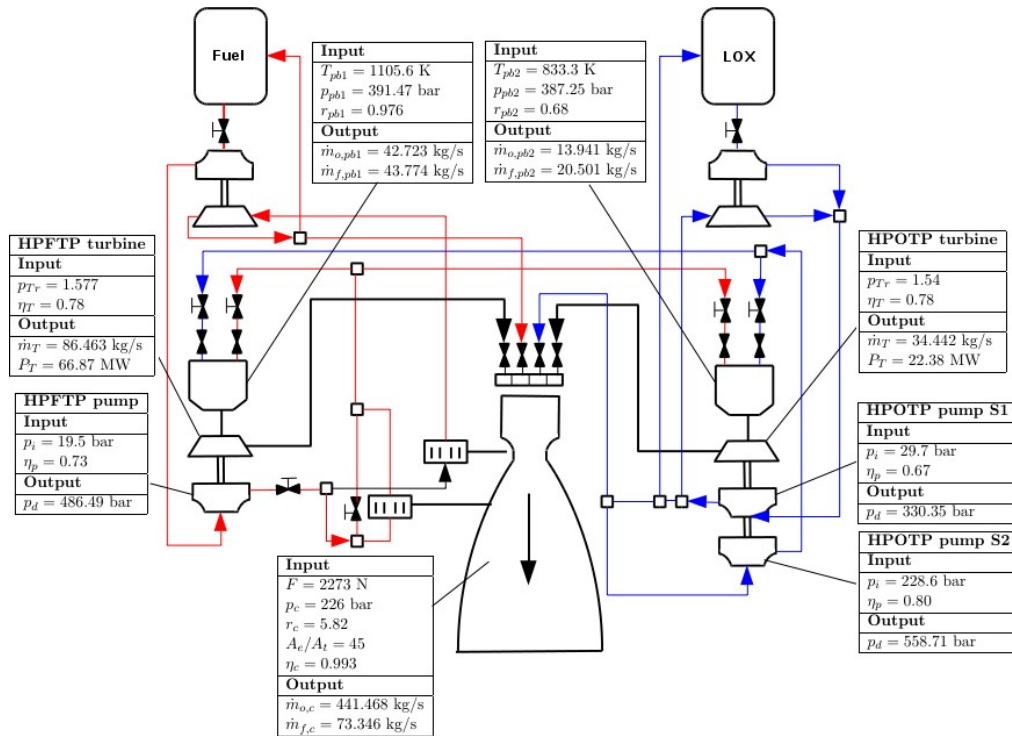


Figure 4. SSME input/output (input data from Manski and Martin 1991).

Table 4. Verification of the simulated parameters of the SSME.

| SSME | Manski and Martin (1991) | Calculated | Error (%) |
|----------------------------|--------------------------|------------|-----------|
| Key input | | | |
| F (kN) | 2273 | – | – |
| p_c (bar) | 219.70 | – | – |
| r_c | 6.019 | – | – |
| A_e / A_t | 77.5 | – | – |
| Output | | | |
| I_{sp} (s) | 444.0 | 451.267 | 1.63 |
| $\dot{m}_{o,pb1}$ (kg/s) | 36.90 | 42.723 | 15.8 |
| $\dot{m}_{f,pb1}$ (kg/s) | 37.81 | 43.774 | 15.8 |
| $\dot{m}_{o,pb2}$ (kg/s) | 13.56 | 13.941 | 2.81 |
| $\dot{m}_{f,pb2}$ (kg/s) | 19.94 | 20.501 | 2.81 |
| $\dot{m}_{T,LPOTP}$ (kg/s) | 83.06 | 82.89 | 0.20 |
| \dot{m}_c (kg/s) | 511.46 | 514.814 | 0.66 |
| $P_{T,HPFTP}$ (MW) | 57.79 | 66.87 | 15.7 |
| $P_{T,HPOTP}$ (MW) | 21.77 | 22.38 | 2.8 |

Apart from the mass flow rate through the fuel pre-burner and the power of the HPFTP turbine ($P_{T,HPFTP}$), all the calculated parameters are very reasonable. The deviations here are due to the same reason presented for the Vulcain engine. The large deviation can be attributed to the fact that Manski and Martin (1991) used an equation function of the enthalpy change to estimate the pump power.

ANALYSIS OF THE L75 ROCKET ENGINE

The analysis of the main parameters of the L75 is presented in this section. To accomplish this task, some considerations must be taken into account, since the engine will work at different operating points (off-design). To this end, the turbine and pump efficiencies, as well as the pressure drop in the feed system, are assumed constant.

The Brazilian L75 rocket engine will work in open cycle with a single shaft turbopump. This is a semi-cryogenic rocket engine that works with liquid oxygen and ethanol. Since the gases expelled by the turbine will be used for thrust vector control (TVC), its contribution to the thrust force is neglected. Figure 5 presents the inputs and outputs used for the engine simulation.

Influence of Chamber Pressure on the Engine Performance

To fulfill this analysis, the thrust is kept constant and the nozzle expansion ratio s varies in order to extract the maximum kinetic energy. Thus, for a pressure vector $p_c = [30 \ 40 \ 50 \ 58.5 \ 80 \ 100]^T$, the values of specific impulse at thrust chamber and nozzle expansion are given in Table 5.

Table 5. Values of specific impulse and nozzle expansion for different chamber pressures.

| L75 Rocket Engine | | | | | | |
|------------------------------|---------|--------|--------|--------|--------|--------|
| p_c (bar) (given) | 30 | 40 | 50 | 58.5 | 80 | 100 |
| Isp(vac) (s) (calculated) | 315.067 | 315.89 | 315.93 | 315.61 | 313.83 | 311.45 |
| A_e / A_t (-) (calculated) | 87.828 | 109.56 | 130.16 | 147 | 187.51 | 223.22 |

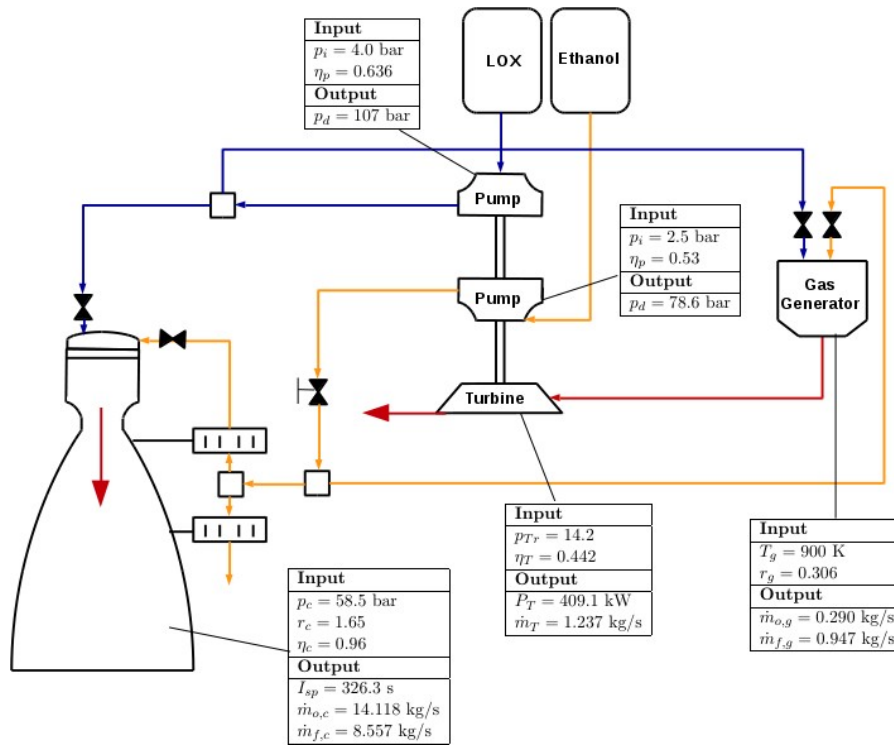


Figure 5. L75 flow scheme with input/output data (input data are courtesy of Brazilian IAE).

To calculate the global specific impulse of the engine we must consider the contribution of the gas generator. The Eq. 25 can be used:

$$I_{sp,oa} = \frac{\dot{m}_g I_{sp,g} + \dot{m}_c I_{sp,c}}{\dot{m}_{ox,oa} + \dot{m}_{fu,oa}} \tag{25}$$

where the subscripts *g*, *c*, and *oa* stands for gas generator, combustion chamber, and overall, respectively. After the simulation of the engine for each chamber pressure, we finally get the results as presented in Fig. 6. The curve profile was as expected for a gas generator cycle. As the chamber pressure increases, the specific impulse at combustion chamber increases, but this is offset with the increased power of the turbine by means of turbine mass flow rate.

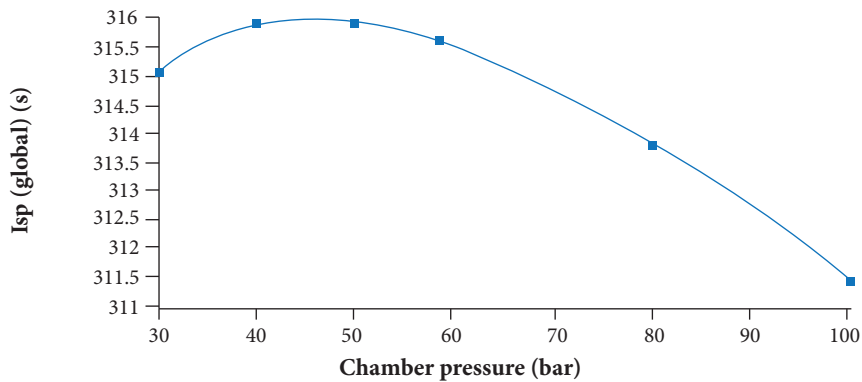


Figure 6. Performance of the L75 rocket engine as function of the chamber pressure.

Influence of Engine Parameters on the Dry Mass

Usually, we are interested in adjusting the design parameters in order to maximize the specific impulse or engine performance. However, conflicting design parameters must also be taken into account. For example, the optimum specific impulse will not necessarily give the minimum engine dry mass or maximum payload mass. Besides, technical issues as the limiting combustion chamber temperature must be pointed out. To assess the dry mass of a liquid rocket engine at different operating points (off-design) some assumptions must be set. To this end, the pump and turbine efficiency, as well as the pressure drop in the feed system, remain constant. Thus, the power of the turbine will be only function of the mass flow rate.

- Step 1: Performance simulation. With the simulation of the engine at different operating points, the mass flow distribution through the engine cycle is determined. Hence, the power of the turbomachinery and the engine performance are obtained.
- Step 2: Dry mass calculation. Making use of the results from the previous item, the engine dry mass can be calculated.

Chamber Pressure

To perform this analysis the nozzle expansion remains constant. Thus, if we choose pressure values of $p_c = [20 \ 30 \ 40 \ 50 \ 58.5 \ 80 \ 100 \ 150 \ 200]^T$, the engine dry mass profile presents a minimum as shown in Fig. 7. This minimum value corresponds exactly to the design point of the L75.

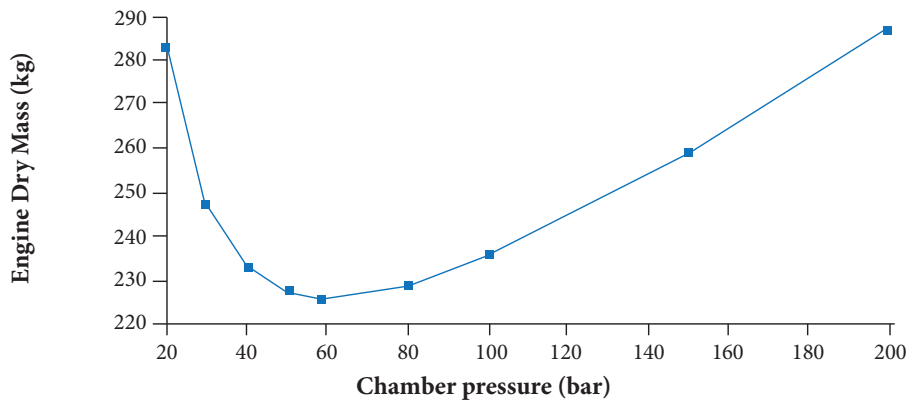


Figure 7. Influence of the chamber pressure p_c on the engine dry mass.

Mixture Ratio

Keeping also the nozzle expansion ratio fixed, if a mixture ratio vector is considered, the engine dry mass profile presents a near optimum value, as shown in Fig. 8.

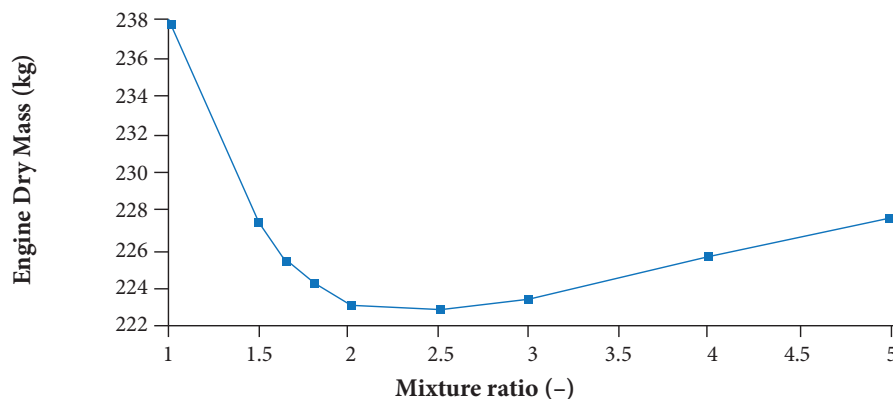


Figure 8. Influence of the mixture ratio r_c on the engine dry mass.

CONCLUSION

An objected-oriented tool for simple analysis of the LOX-Ethanol liquid rocket engine was presented. Mathematical models comprising the main components of a liquid rocket engine and cycle balance were presented. The UML tool was chosen to model the architecture of the codes. UML diagrams help to visualize the structure of the codes and communication between objects. Furthermore, these diagrams provide a high degree of abstraction, i.e., only the relevant functionality of the codes is explicit to the user. Thus, anyone that has some acquaintance with object-oriented can easily understand the main functions and parameters of each single class as well as the relationship between objects. To verify the applicability and efficiency of the engine performance codes, the liquid rocket engines Vulcain, HM7B, and SSME were simulated. As expected, appropriate caution must be taken in estimating the pump performance if we are dealing with low-density propellants (mainly liquid hydrogen) under extremely high pressures. In other words, considerable discrepancies in estimating the pump power can be found if an equation derived for constant density is used. By varying the mixture ratio and chamber pressure of the L75, near optimum values were determined. Thus, we can see that an optimal compromise between minimum dry mass and maximum performance must be fulfilled. For an open cycle liquid rocket engine, when the chamber pressure is increased in order to increase the performance, the turbine requires more power, which means greater mass flow rate through the turbine, so the near optimum global specific impulse is due to the contribution of propellant energy used to drive turbine. The model cycle used in this work had maximum error of: 7.6% in Vulcain fuel turbine power, 1.68% in HM7B turbine power, and approximately 15.8% in SSME mass flow in the pre-burner of the fuel side. This can be explained due to fluids with low densities do not behave exactly like incompressible fluid under extremely high pressure. But for the specific impulse a maximum error of 1,63% was achieved in SSME LRE, this level of error is expected in the L75 LRE specific impulse analysis.

AUTHOR'S CONTRIBUTION

Conceptualization, Mota FAS, Hinckel JN and Rocco EM; Methodology, Mota FAS, Hinckel JN and Schlingloff H; Writing – Original Draft, Mota FAS; Writing – Review & Editing, Mota FAS, Hinckel JN, Rocco EM and Schlingloff H.

REFERENCES

- Burkhardt H, Sippel M, Herberth A, Klevanski J (2002) Comparative study of kerosene and methane propellant engines for reusable liquid booster stages. Presented at: 4th International Conference on Launcher Technology "Space Launcher Liquid Propulsion"; Liège, Belgium.
- Burkhardt H, Sippel M, Herberth A, Klevanski J (2004) Kerosene vs. methane: a propellant tradeoff for reusable liquid booster stages. *Journal of Spacecraft and Rockets* 41(5):762-769. doi: 10.2514/1.2672
- Castellini F (2012) Multidisciplinary design optimization for expendable launch vehicles (PhD thesis). Milan: Politecnico Di Milano.
- Ernst RRL (2014) Liquid Rocket Analysis (LiRA): development of a liquid bi-propellant rocket engine design, analysis and optimization tool (Master's Dissertation). Delft: Delft University of Technology.
- Felber R (1979) Einige Beiträge Zur Optimierung von Chemischen Raketentriebwerken. Munich: University of Munich. In German.
- Goertz C (1995) A modular method for the analysis of liquid rocket engine cycles. Presented at: 31st Joint Propulsion Conference and Exhibit; San Diego, USA. doi: 10.2514/6.1995-2966
- Gordon S, McBride BJ (1994) Computer program for calculation of complex chemical equilibrium compositions and applications. Part 1: analysis. (NASA-RP-1311) NASA Technical Report.
- Gordon S, McBride BJ (1996) Computer program for calculation of complex chemical equilibrium compositions and applications. Part 2: users manual and program description. (NASA-RP-1311-P2) NASA Technical Report.

- Hinckel J (1995) An object oriented approach to launch vehicle performance analysis. Presented at: 31st Joint Propulsion Conference and Exhibit; San Diego, USA. doi: 10.2514/6.1995-3094
- Humble RW, Henry GN, Larson WJ (1995) Space propulsion analysis and design. New York: McGraw-Hill.
- Huzel DK, Huang, DH (1992) Modern engineering for design of liquid-propellant rocket engines. Washington DC: AIAA.
- Kauffmann J, Herbertz A, Sippel M (2001) Systems analysis of a high thrust, low-cost rocket engine. Presented at: 4th International Conference on Green Propellants for Space Propulsion; Noordwijk, Netherlands.
- Kesaev KhV, Almeida DS (2005) Teoria e cálculo de motores foguete a propelente líquido. IAE Internal Report. In Portuguese.
- Manski D, Goertz C, Saßnick H, Hulka JR, Goracke BD, Levack DJH (1998) Cycles for Earth-to-orbit propulsion. Journal of Propulsion and Power 14(5):588-604. doi: 10.2514/2.5351
- Manski D, Martin J (1990) Optimization of the propulsion cycles for advanced shuttles. Part 2: performance model methodology. Presented at: 26th Joint Propulsion Conference; Orlando, USA. doi: 10.2514/6.1990-2436
- Manski D, Martin JA (1991) Evaluation of innovative rocket engines for single-stage Earth-to-orbit vehicles. Journal of Propulsion and Power 7(6):929-937. doi: 10.2514/3.23411
- Mc Hugh B (1995) Numerical analysis of existing liquid rocket engines as a design process starter. Presented at: 31st Joint Propulsion Conference and Exhibit; San Diego, USA. doi: 10.2514/6.1995-2970
- Pavli AJ, Curley JK (1996) Design and cooling performance of a dump-cooled rocket engine. (NASA-TN-D-3532). NASA Technical Note.
- Pouliquen MF (1984) HM60 cryogenic rocket engine for future European launchers. Journal of Spacecraft and Rockets 21(4):346-353. doi: 10.2514/3.25661
- Press WH, Teulolsky SA, Vetterling WT, Flannery BP (2007) Numerical recipes: the art of scientific computing. Cambridge: Cambridge University Press.
- Schlingloff H (2005) Astronautical engineering: an introduction to the technology of spaceflight. Bad Abbach: Ingenieurbuero Dr. Schlingloff Publications.
- Sippel M, Herbertz A, Manfletti C, Burkhardt H, Imoto T, Haeseler D, Götz A (2003) Studies on expander bleed cycle engines for launchers. Presented at: 39th Joint Propulsion Conference and Exhibit; Huntsville, USA. doi: 10.2514/6.2003-4597
- Sippel M, Yamashiro R, Cremaschi F (2012) staged combustion cycle rocket engine design trade-offs for future advanced passenger transport. Presented at: Space Propulsion Bourdeaux, France.
- Sutton GP, Biblarz O (2010) Rocket Propulsion Elements. New Jersey: John Wiley.
- White FM (1998) Fluid Mechanics. 4th ed. New York: McGraw-Hill.
- Zandbergen B (2013) Simple mass and size estimation relationships of pump fed rocket engines. Delft University of Technology Technical Report.